Journal of Physical Science, Vol. 33(2), 61–75, 2022

Compatibility of Concentrated NaOH as a Precipitation Agent in the Synthesis of Maghemite (γ-Fe_2O_3) Nanoparticles via Co-precipitation Method

Hamisah Ismail,[1,2] Zalita Zainuddin,[1] Hasmaliza Mohamad[2] and Muhammad Azmi Abdul Hamid[1*]

[1]School of Applied Physics, Faculty of Science and Technology, Universiti Kebangsaan Malaysia, 43600 UKM Bangi, Selangor, Malaysia
[2]School of Materials and Mineral Resources Engineering, Universiti Sains Malaysia, 14300 Nibong Tebal, Pulau Pinang, Malaysia

[*]Corresponding author: azmi@ukm.edu.my

Published online: 25 August 2022

To cite this article: Hamisah, I. et al. (2022). Compatibility of concentrated NaOH as a precipitation agent in the synthesis of maghemite (γ-Fe_2O_3) nanoparticles via co-precipitation method. *J. Phys. Sci.*, 33(2), 61–75. https://doi.org/10.21315/jps2022.33.2.4

To link to this article: https://doi.org/10.21315/jps2022.33.2.4

ABSTRACT: *Maghemite (γ-Fe_2O_3) nanoparticles were synthesised using the co-precipitation method, with different concentrations (5 M, 10 M, 11 M, 12 M and 13.4 M) of sodium hydroxide (NaOH) as the precipitation agent. The resulting powder was characterised using x-ray diffraction (XRD), vibrating sample magnetometer (VSM), and transmission electron microscope (TEM). All characterisations were performed at room temperature. The XRD results showed that the γ-Fe_2O_3 powder was in a single phase for samples synthesised using 11 M, 12 M and 13.4 M NaOH and the crystallite size ranged between 5.74 nm–6.42 nm. TEM observations and analysis showed that the particles were in a cubo-spheroidal shape and the mean physical size of the nanoparticles was between 8.52 nm and 8.59 nm. Hysteresis loop indicated that γ-Fe_2O_3 nanoparticles have superparamagnetic properties with an acceptable range of saturation magnetisation of 31.08 emu/g–48.88 emu/g and negligible coercivity value. MTT assay demonstrated that the γ-Fe_2O_3 nanoparticles exhibited biocompatibility with V79-4 cells at different dosages (1000 μg/mL–50 μg/mL) for 48 h. The results suggested that maghemite can be a valuable low-cost biomagnetic material in biomedical applications.*

Keywords: biocompatibility, co-precipitation method, maghemite nanoparticle, superparamagnetic

1. INTRODUCTION

The synthesis of nano-sized magnetic materials has recently become an area of interest. The development of metal oxides has been intensively studied due to the importance of nano-sized materials. Magnetic nanoparticles often show fascinating magnetic, chemical, electrical and optical properties, which surpass their bulk counterparts.[1] Some magnetic materials are biocompatible, non-toxic, physically and chemically stable, environmentally safe and able to form stable dispersions. Therefore, they are suitable for different biomedical applications, such as MRI contrast agents, drug delivery, cancer treatment using magnetic hyperthermia, immunoassay, cancer theranostics and other applications in different fields, including catalysis.[2–7] The synthesis of iron oxide and ferrite oxide is of great interest because they can store information nanotechnology as magnetic resonance agents such as, ferrous fluids and in catalysis.[8–10] Because of their polymorphism and temperature-induced phase transition, three well-known iron oxides namely, hematite (α-Fe_2O_3), magnetite (Fe_3O_4) and maghemite (γ-Fe_2O_3), are highly sought after. These iron oxides have distinct magnetic, biochemical and biocompatible properties that make them suitable for biomedical applications. Maghemite is one of the most attractive iron oxides due to its excellent chemical stability and heating capability.[11] It is effective for various applications such as for developing synthetic pigments, recording materials, wastewater treatment and fusion fluid technology.[12] Magnetic fluid hyperthermia using superparamagnetic iron oxide nanoparticles has recently became a breakthrough approach in cancer treatments.[13,14] Because surface effects could reduce saturation magnetisation in tiny magnetic nanoparticles which indirectly affects the specific loss power (SLP) value, different coatings have been used for the superparamagnetic iron oxide nanoparticles to improve their efficiency while maintaining stability and biocompatibility.[14] For an efficient heavy metal adsorption, iron oxide-based magnetic nanoparticles with large specific surface areas were successfully prepared in a previous study.[15] Magnetic nanoparticles with high magnetisations were obtained because of their small dimensions and superparamagnetic behaviour. The synthesising procedures were meticulously controlled, allowing for efficient separation with a single magnet while avoiding irreversible aggregation. As a result, the magnetic nanoadsorbents designed in this study have high surface areas, colloidal stability and magnetism that can be used to treat industrial wastewater and in other environmental applications.[15]

Maghemite has attracted researchers' attention because it has unique characteristics, such as non-toxic, functional harmony, thermal and chemical stability and beneficial hysteresis properties. It is seen as a valuable material when combined with biologically active compounds, drug biomolecules and localised heating of cancer cells, among others.[16,17] It also has a chemically active surface where various bonds can be formed, which allows coatings to be created from multiple bioactive molecules.[12]

Hematite is the most stable iron oxide under environmental conditions and has n-type semiconductor properties. Because of its low cost and high corrosion resistance, it is widely used in magnetic membranes, pigments, gas sensors and catalysts. It can also be used as a precursor in the synthesis of magnetite and maghemite, both of which have been actively pursued in recent years for critical scientific interests, as well as technological needs.[18]

The most common precursor materials for the synthesis of maghemite are ferric (II) chloride tetrahydrate ($FeCl_2 \cdot 4H_2O$), ferric (III) chloride hexahydrate ($FeCl_3 \cdot 6H_2O$) and ferric nitrate nonahydrate ($Fe(NO_3)_3 \cdot 9H_2O$).[11,19,20] Various methods and techniques have been reported for the synthesis of iron oxide nanoparticles, such as co-precipitation, hydrothermal, sol-gel, microemulsion, thermal decomposition, biosynthesis and ball mill.[7,11,21–26] The behaviour of these magnetic materials relies on their chemical composition, preparation and particle size.[27,28] Co-precipitation is a versatile, simple and low-cost method for producing high-yield iron oxide nanoparticles.

In this study, the co-precipitation method was modified by using different concentrations of sodium hydroxide (NaOH) as the precipitation agent compared to the commonly used 25% of concentrated ammonia (NH_3).[11,29] The main factor in selecting NaOH as the precipitation agent was that it is less harmful, easy to handle and has no strong odour like ammonia. Different NaOH concentrations at 5 M, 10 M, 11 M, 12 M and 13.4 M, and 25% of 13.4 M NH_3 were used to produce maghemite nanoparticles. The aeration process was applied in this study to produce maghemite nanoparticles from the Fe_3O_4 phase. This method is advantageous because no surfactant has to be removed from the nanoparticles prior to being used in an application. Several characterisations were conducted, such as phase analysis, magnetic test, particle size determination, morphology study and cytocompatibility to determine the efficacy of the concentrated NaOH to produce the desired material.

2. MATERIALS AND METHOD

The starting materials for the synthesis of maghemite nanoparticles included iron (II) chloride ($FeCl_2$, 98%, Sigma Aldrich), iron (III) chloride ($FeCl_3$, 97%, Sigma Aldrich), hydrochloric acid (HCl, 37%, Merck) and sodium hydroxide (NaOH, 99%, R&M Chemicals). Deionised water was used throughout the experiments.

Maghemite nanoparticles were synthesised using a chemical co-precipitation technique. In this study, 2.08 g of $FeCl_2$ and 5.22 g of $FeCl_3$ in powder form were dissolved in 380 mL of deionised water. Appropriate amounts of both solutions were mixed in a beaker and stirred using a magnetic stirrer at 500 rpm on a hot plate at room temperature. After the powders have dissolved, 10 mL of 2 M HCl was added to the solution to prevent Fe^{2+} oxidation and Fe^{3+} precipitation in the form of hydroxide. Then, 20 mL of NaOH at different concentrations (5 M, 10 M, 11 M, 12 M and 13.4 M) was added separately and stirred for 30 min. The selection of NaOH concentrations was made based on the NH_3 concentration used by Ewijk et al. (1999), which was 20 mL of 25% NH_3 that equals to 13.4 M when converted to molarity.[29] To produce maghemite nanoparticles, the solution was heated up to 100°C and continuously stirred for 30 min on a hot plate. Then, the solution was cooled to room temperature before undergoing the centrifugation process for four consecutive times using deionised water at 10,000 rpm for 15 min. The resultant precipitate was washed with deionised water to eliminate as many residual chlorides as possible. The resultant slurries, as shown in Figure 1, are dried in an oven at 50°C for two days before characterisation analysis was conducted.

Figure 1: Sample solution as prepared: (a) post synthesis, (b) maghemite solution pre-centrifugation and (c) maghemite suspension post-centrifugation.

The formed nanoparticles were characterised using an x-ray diffractometer (XRD, D8 Advance, Bruker, Germany) with a Cu Kα radiation source. XRD data were obtained from 10°–80°, using a step scan of 0.03°. The average crystallite size of the as-prepared particles was calculated using the following Scherrer equation:

$$L = K\lambda / \beta \cos \theta \quad (1)$$

where L is the size of the crystallite (nm), K is Scherrer's constant, λ is the x-ray wavelength, β is the full width at half maximum (FWHM) in radian after correction for instrumental peak broadening, and theta (θ) is the Bragg angle. In this calculation, the K value was 0.94.

The magnetisation measurements were directly performed on the synthesised powder using a vibrating sample magnetometer (VSM, Lakeshore 7410, USA) at room temperature. A transmission electron microscope was used to photograph the resulting maghemite powder (TEM, Philips CM200). The powdered samples were dispersed in ethanol using ultrasonication, and a drop of the dispersion material was placed on a 300-mesh carbon-coated Cu grid. The Image-J software calculated the size distribution and average diameters for up to 100 particles.

The maghemite powder and V79-4 cells were used to perform cytotoxicity evaluation via the MTT assay method by referring to the standard of ISO 10993-5:2009. The V79-4 cells were grown in tissue culture flasks using Dulbecco's Modified Eagle Medium (DMEM). It was supplemented with 10% of fetal bovine serum, 1 mM sodium pyruvate and 1% of antibiotics (penicillin and streptomycin) as the complete growth medium at 37°C in a humidified atmosphere of 5% CO_2 and 95% air. Trypsinisation was used to remove the confluent monolayer and the number of viable cells was determined. Cells were seeded at a density of 10,000 cells per well in a 96-well plate and incubated at 37°C for at least 12 h. The test material that consisted of maghemite powders was made by extracting it with a complete growth medium at the highest concentration of 200 mg/mL in a shaking water bath for 24 h at 37°C. The extracted maghemite was sterilised using a membrane filtration method and serially diluted into five percentage concentrations of 3.13%, 6.25%, 12.5%, 25% and 50% before being tested in triplicate. Each well of a 96-well plate containing healthy culture had its growth medium replaced with 200 µl of maghemite extract or controls.

A cytotoxic effect is defined as a decrease in cell viability that is greater than 30%. Cell viability was calculated using the mean, standard deviation and percentage. Equation 2 was used to determine the percentage of inhibition:

$$\% \text{ cell viability} = \frac{\text{Mean OD test material}}{\text{Mean OD negative comtrol}} \times 100 \quad (2)$$

3. RESULTS AND DISCUSSION

NaOH was used to investigate the effect of an alkaline precipitation agent at different molarities during precipitation. When NaOH was added at the start of the co-precipitation, it immediately supplied hydroxide ($–OH^-$) ions, which raised the pH of the reaction and created a highly reducing environment. Higher pH values immensely helped in the instantaneous precipitation of the Fe^{2+} and Fe^{3+} ions. In the initial synthesis of maghemite, optimum aeration temperature, stirring speed and stoichiometric ratio of iron salts in the presence of alkali were encouraged. The addition of high molarity alkali, combined with vigorous stirring, aided in forming maghemite nanoparticles. The immediate dissolution of the iron salts in boiling water increased their activity, and vigorous stirring ensured a consistent and uniform nucleation environment.

Changes in pH were measured due to different molarity concentrations used to synthesise maghemite. When $FeCl_2$ and $FeCl_3$ were mixed in deionised water, the colour of the solution turned yellowish, and the pH value was recorded at 0.7–0.8. Next, when HCl was poured into the mixture, the yellow colour turned into a lighter yellow, with a pH value of 0.6–0.7. While pouring the 5 M NaOH, the colour of the mixture became light brown, and the pH reading was 3.6 until the aeration process was finished, with a pH reading of 0.5. These changes showed that no magnetite (Fe_3O_4) phase was formed. Previous studies reported that once the precipitation agent (e.g., ammonia) was poured, the yellow solution turned black.[30,31]

When high concentrations were used, starting at 10 M, 11 M, 12 M and 13.4 M NaOH, the pH was approximately 12.45–13.00. The mixture turned completely black for all concentrations, thus, confirming the presence of the hematite phase. Then, 30 min after the aeration process, the pH was decreased to 10.45, 9.9, 9.6 and 8.5 with 10 M, 11 M, 12 M and 13.4 M NaOH, respectively. The subsequent colour for all concentrations was dark brown. A summary of pH values for the different NaOH concentrations during synthesis is shown in Table 1. This table shows that higher NaOH concentrations of 11 M, 12 M and 13.4 M produced better formed maghemite particles.

Table 1: Values of pH with the addition of NaOH and after 30 min of aeration during synthesis

Activity	Concentration of NaOH (M)				
	5	10	11	12	13.4
After NaOH addition	3.60	12.45	12.54	12.65	13.00
30 minutes after aeration process	0.5	10.4	9.9	9.6	8.5

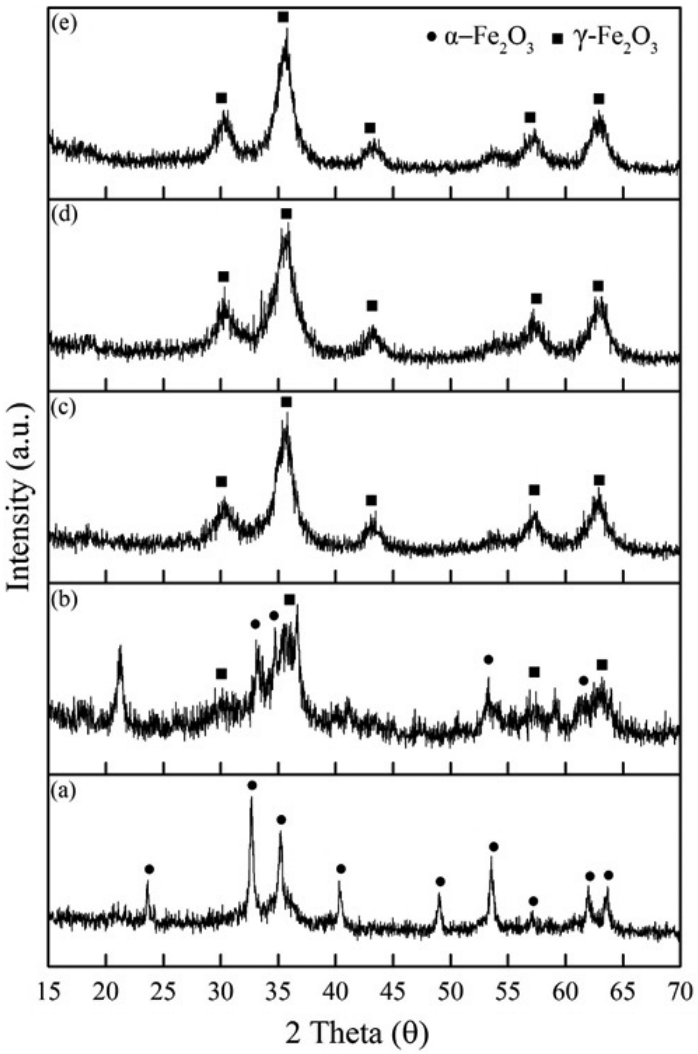

Figure 2: X-ray patterns of nanoparticles obtained using the co-precipitation method.

Figure 2 shows the XRD patterns of five samples prepared at different NaOH concentrations. In Figure 2(c–e), the presence of single-phase maghemite (γ-Fe_2O_3) (JCPDS 39-1346) is confirmed, with peaks corresponding to the 220, 311, 400, 422, 511 and 440 planes for samples added with 11 M, 12 M and 13.4 M NaOH. A single phase of hematite (α-Fe_2O_3) (JCPDS 33-0664) is detected at the low concentration of 5 M NaOH, with peaks corresponding to the 012, 104, 110, 113, 024, 116, 118, 214 and 441 planes, as shown in Figure 2(a). However, for 10 M NaOH, a mixed phase of maghemite and hematite is discovered (as shown in Figure 2[b]). The formation of maghemite and hematite phases can be affected by a high or low NaOH molarity. The discovery made by Saxena and Singh supported this finding, whereby nanocrystalline particles with a large surface area are more likely to oxidise, resulting in the formation of maghemite.[32] Lower alkali concentrations have frequently resulted in a higher percentage of magnetite (Fe_3O_4).

The sizes of maghemite nanoparticles synthesised using 11 M, 12 M and 13.4 M NaOH in this experiment conformed to the size range of superparamagnetic particles. Table 2 shows the average sizes of the crystallites, as determined using the Scherrer equation, based on the highest peak for all samples. The average crystallite size ranged between 5 nm and 30 nm for all NaOH concentrations in this study.

Table 2: Effect of different NaOH concentrations on the crystallite size of maghemite synthesised via co-precipitation.

Concentration (M)	5	10	11	12	13.4
Crystallite size (nm)	28.8	19.6	5.7	5.7	6.4

The VSM study was conducted at room temperature from −14 kOe to +14 kOe to evaluate the magnetic properties of the nanoparticles. All samples produce non-linear reversible graphs with insignificant retentivity and coercivity values, as shown in Figure 3. The resultant nanoparticles exhibited superparamagnetic behaviour, with higher saturation magnetisation values compared to those reported by other researchers.[33,34] Figure 3 shows the typical magnetisation curves and hysteresis loops for the synthesised maghemite and hematite nanoparticles. Table 3 lists the experimental magnetic properties of the nanoparticles.

Table 3: Magnetic properties of the synthesised nanoparticles.

Samples (M)	Saturation magnetisation (Ms) (emu/g)	Coercivity (Hc) (G)	Retentivity (Mr) (emu/g)
5	2.79	8.94	7.28×10^{-3}
11	32.29	0.267	6.76×10^{-3}
12	31.08	0.31	7.74×10^{-3}
13.4	48.88	0.70	6.18×10^{-3}

The saturation magnetisation values and magnetic parameters of maghemite nanoparticles are affected by several factors, including the synthesis procedure, crystallinity, particle size, surface structure and crystal defects.[32] The magnetic properties of the comparable size and particle size distribution depend significantly on the crystallinity and surface properties of the particles.

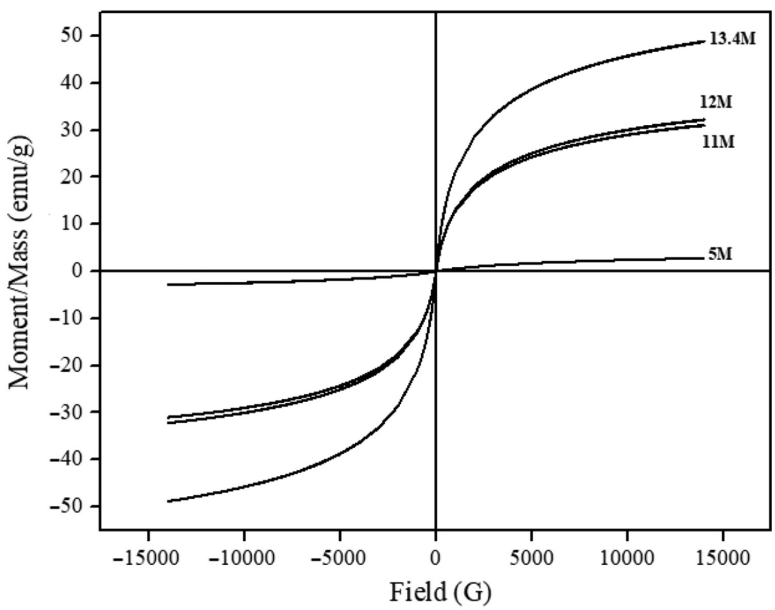

Figure 3: Magnetisation curves for nanoparticles synthesised using different NaOH concentrations measured at room temperature.

TEM micrographs of samples synthesised using 11 M and 12 M NaOH are shown in Figures 4 and 5, respectively, to confirm the crystallite size and maghemite presence. The resultant nanoparticles were well dispersed and agglomerated. Most nanoparticles are cubo-spheroidal in shape, as shown in Figures 4(a) and 5(a). The size distribution curve shows that these

nanoparticles are approximately 8–10 nm (11 M NaOH) and 6–10 nm (12 M NaOH) in size, with narrow size distribution and mean size of 8.59 nm and 8.52 nm, respectively (as shown in Figures 4[b] and 5[b]). In conclusion, these two samples showed that the shape and size of maghemite nanoparticles were almost similar and fit the size range of superparamagnetic particles.

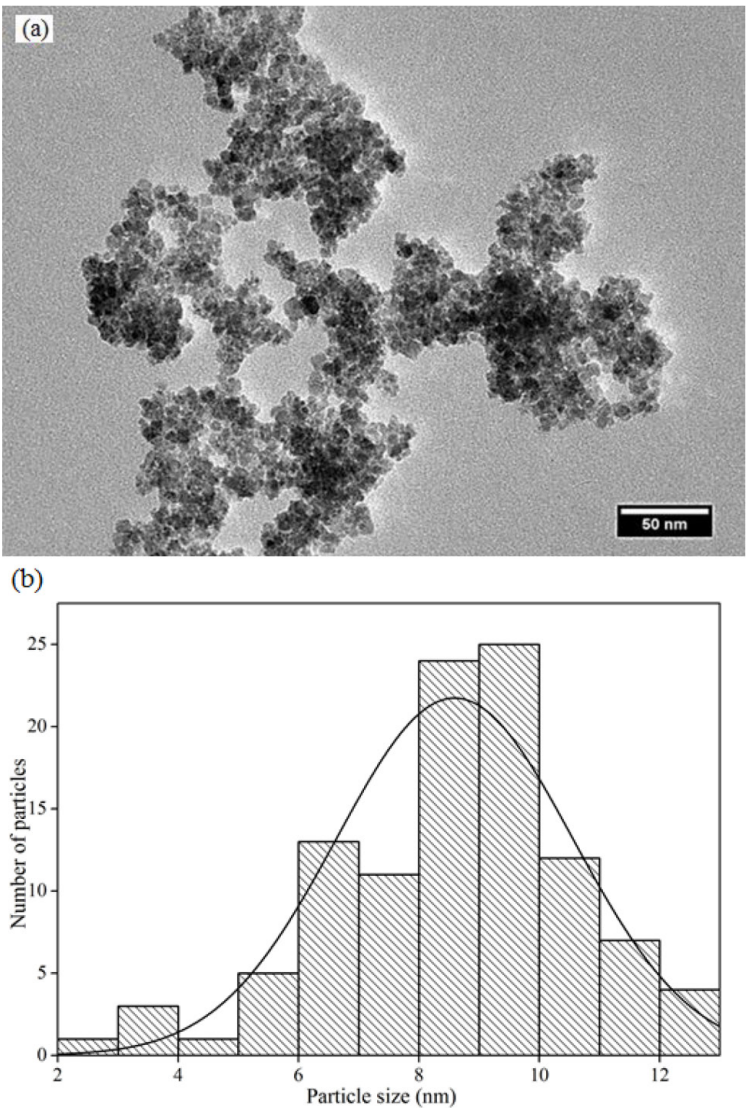

Figure 4: (a) TEM image of maghemite (γ-Fe_2O_3) synthesised using 11 M NaOH and (b) size distribution and average diameters.

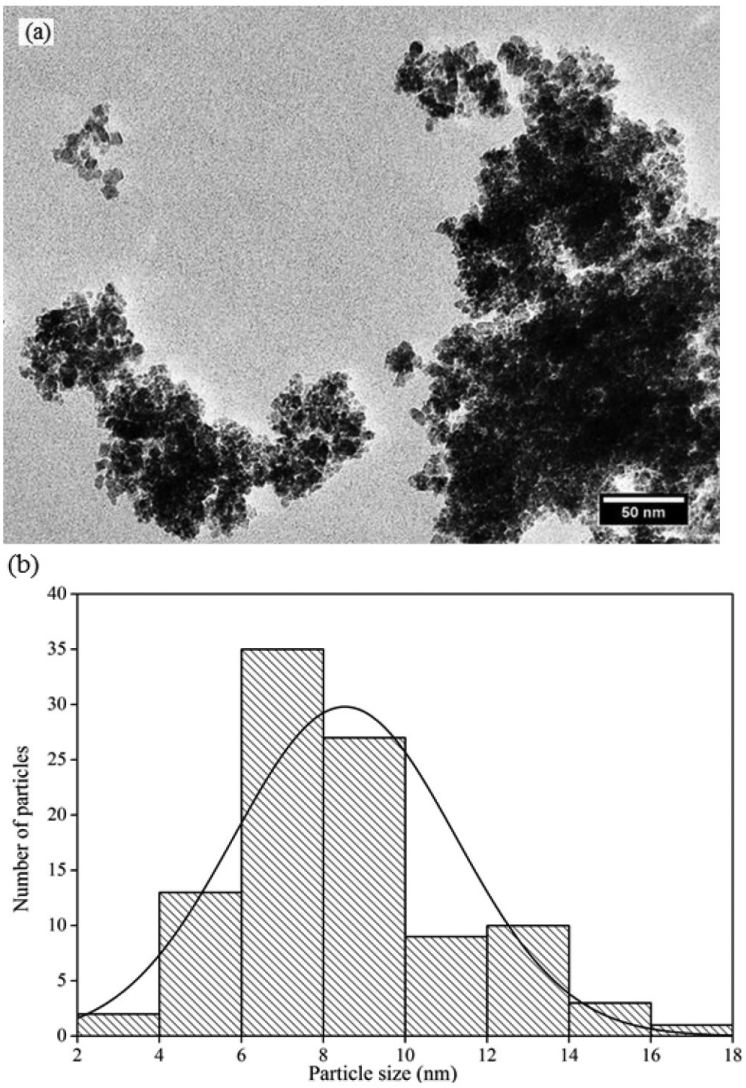

Figure 5: (a) TEM image of maghemite (γ-Fe_2O_3) synthesis using 12 M NaOH and (b) size distribution and average diameters.

A biocompatibility study of the 12 M NaOH powders using the MTT assay method was successfully performed based on the viability of cells. The cytotoxicity was determined by assessing cell viability by reducing tetrazolium salts (MTT). As shown in Figure 6, no significant change is observed in V79-4 cell viability at different dosages from 3.13 μg/mL to 100 μg/mL after 24 h of exposure. Thus, the tested maghemite extract did not inhibit

the viability of V79-4 cells at any of the concentrations tested according to ISO 10993-5:2009 criteria. Under the conditions of this study, maghemite powders had no cytotoxic effect. Both negative (complete growth medium) and positive control (zinc diethyldithiocarbamate) were performed as anticipated. Hence, the biocompatibility test confirmed that the synthesised maghemite has no biological cell toxicity; consequently, it can have a significantly active role in biological applications.

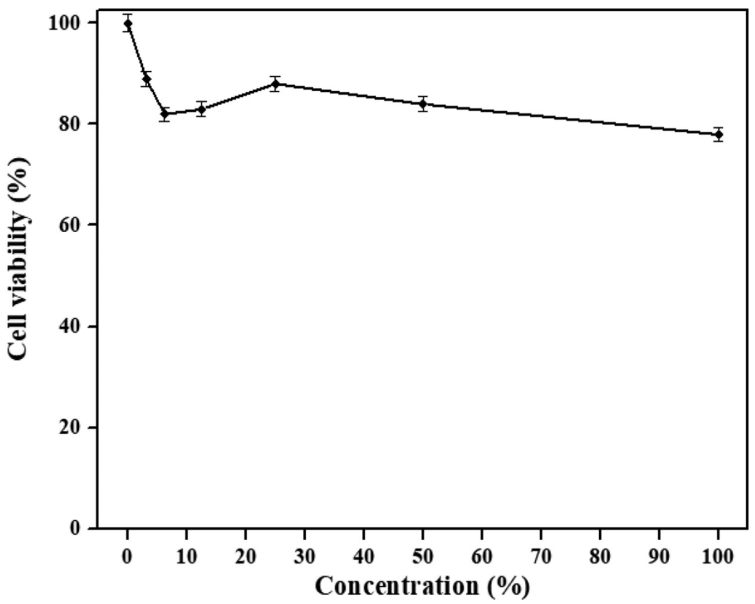

Figure 6: Cell viability of maghemite with V79-4 cells using MTT assay.

4. CONCLUSION

It has been concluded that maghemite (γ-Fe_2O_3) was successfully synthesised using 11 M, 12 M and 13.4 M NaOH via the co-precipitation method. Analysis results proved that NaOH molarities of 11 M, 12 M and 13.4 M were optimum for the single-phase formation of maghemite. XRD and TEM analyses confirmed the presence of maghemite with small particle sizes ranging between 6 nm and 10 nm for the 11 M and 12 M samples. The resultant particle shape was cubo-spheroidal, with excellent superparamagnetic properties and no cytotoxicity, applicable in the biomedical field. Further studies are in progress to investigate the role of maghemite nanoparticles doped into bioceramic materials for the scaffold.

5. ACKNOWLEDGEMENTS

The authors would like to express their gratitude to Associate Professor Dr Roslinda Shamsudin for her valuable and constructive suggestions during the planning and development phase of this research work. This work is supported by the DCP-2017-001/1 research grant. The authors would also like to thank the Ministry of Higher Education Malaysia, the Faculty of Science and Technology, CRIM and Makmal Bioserasi Universiti Kebangsaan Malaysia for supporting this research.

6. REFERENCES

1. Issa, B. et al. (2013). Magnetic nanoparticles: Surface effects and properties related to biomedicine applications. *Int. J. Mol. Sci.*, 14(11), 21266–21305. https://doi.org/10.3390/ijms141121266
2. Huang, D. M. et al. (2009). The promotion of human mesenchymal stem cell proliferation by superparamagnetic iron oxide nanoparticles. *Biomaterials*, 30(22), 3645–3651. https://doi.org/10.1016/j.biomaterials.2009.03.032
3. Wahajuddin & Arora, S. (2012). Superparamagnetic iron oxide nanoparticles: Magnetic nanoplatforms as drug carriers. *Int. J. Nanomed.*, 7, 3445–3471. https://doi.org/10.2147/IJN.S30320
4. Tampieri, A. et al. (2012). Intrinsic magnetism and hyperthermia in bioactive Fe-doped hydroxyapatite. *Acta Biomater.*, 8(2), 843–851. https://doi.org/10 .1016/j.actbio.2011.09.032
5. Tanaka, T. & Matsunaga T. (2000). Fully automated chemiluminescence immunoassay of insulin using antibody – protein A – bacterial magnetic particle complexes. *Anal. Chem.*, 72(15), 3518–3522. https://doi.org/10.1021/ac9912505
6. Hajba, L. & Guttman, A. (2016). The use of magnetic nanoparticles in cancer theranostics: Toward handheld diagnostic devices. *Biotechnol. Adv.*, 34(4), 354–361. https://doi.org/10.1016/j.biotechadv.2016.02.001
7. Abu-Dief, A. M. & Abdel-Fatah, S. M. (2018). Development and functionalization of magnetic nanoparticles as powerful and green catalysts for organic synthesis. *Beni-Suef Univ. J. Basic Appl. Sci.*, (7)1, 55–67. https://doi.org/ 10.1016/j.bjbas.2017.05.008
8. Sun, Y. et al. (2005). An improved way to prepare superparamagnetic magnetite-silica core-shell nanoparticles for possible biological application. *J. Magn. Magn. Mater.*, 285(1–2), 65–70. https://doi.org/10.1016/j.jmmm.2004 .07.016
9. Veintemillas-Verdaguer, S. et al. (2004). Colloidal dispersions of maghemite nanoparticles produced by laser pyrolysis with application as NMR contrast agents. *J. Phys. D Appl. Phys.*, 37(15), 2054–2059. https://doi.org/10.1088/ 0022-3727/37/15/002

10. Islam, S. et al. (2014). Simple hydrothermal synthesis and morphological study of magnetic nanoparticles. *J. Nanosci. Nanoeng. Appl.*, 4(2), 14–22.
11. Wu, Z. G. & Gao, J. F. (2012). Synthesis of γ-Fe_2O_3 nanoparticles by homogeneous co-precipitation method. *Micro Nano Lett.*, 7(6), 533–535. https://doi.org/10.1049/mnl.2012.0310
12. Cornell, R. M. & Schwertmann, U. (2003). *The iron oxides: Structure, properties, reactions, occurences and uses*. Weinheim: WILEY-VCH Verlag GmbH & Co.
13. Das, P. et al. (2019). Recent advances in magnetic fluid hyperthermia for cancer therapy. *Colloids Surf. B Biointerfaces*, 174, 42–55. https://doi.org/10.1016/j.colsurfb.2018.10.051
14. Hajalilou, A. et al. (2021). Superparamagnetic Ag-Fe_3O_4 composites nanoparticles for magnetic fluid hyperthermia. *J. Magn. Magn. Mater.*, 537, 168242. https://doi.org/10.1016/j.jmmm.2021.168242
15. Pardo, A. et al. (2021). Monodisperse superparamagnetic nanoparticles separation adsorbents for high-yield removal of arsenic and/or mercury metals in aqueous media. *J. Mol. Liq.*, 335, 116485. https://doi.org/10.1016/j.molliq.2021.116485
16. Mahmoudi, M. et al. (2009). Cell toxicity of superparamagnetic iron oxide nanoparticles. *J. Colloid Interface Sci.*, 336(2), 510–518. https://doi.org/10.1016/j.jcis.2009.04.046
17. Ngadiman, N. et al. (2015). γ-Fe_2O_3 nanoparticles filled polyvinyl alcohol as potential biomaterial for tissue engineering scaffold. *J. Mech. Behav. Biomed. Mater.*, 49, 90–104. https://doi.org/10.1016/j.jmbbm.2015.04.029
18. Kaco, H. et al. (2017). Preparation and characterization of Fe_3O_4/regenerated cellulose membrane. *Sains Malays.*, 46(4), 623–628. https://doi.org/10.17576/jsm-2017-4604-15
19. Darezereshki, E. et al. (2010). One-step synthesis of maghemite (γ-Fe_2O_3) nano-particles by wet chemical method. *J. Alloys. Compd.*, 502(1), 257–260. https://doi.org/10.1016/j.jallcom.2010.04.163
20. Subbiahdoss, G. et al. (2012). Magnetic targeting of surface-modified superparamagnetic iron oxide nanoparticles yields antibacterial efficacy against biofilms of gentamicin-resistant staphylococci. *Acta Biomater.*, 8(6), 2047–2055. https://doi.org/10.1016/j.actbio.2012.03.002
21. Horner, O. et al. (2009). Hydrothermal synthesis of large maghemite nanoparticles: Influence of the pH on the particle size. *J. Nanoparticle Res.*, 11, 1247–1250. https://doi.org/10.1007/s11051-008-9582-x
22. Lau, L. N. & Ibrahim, N. B. (2015). Characterizations of maghemite thin films prepared by a sol-gel method. *AIP Conf. Proc.*, 1678(1), 040013. https://doi.org/10.1063/1.4931270
23. Nurdin, I. et al. (2014). Synthesis, characterisation and stability of superparamagnetic maghemite nanoparticle suspension. *Mater. Res. Innov.*, 18, 200–203. https://doi.org/10.1179/1432891714Z.0000000001017

24. Aliahmad, M. & Nasiri, M. N. (2013). Synthesis of maghemite (γ-Fe_2O_3) nanoparticles by thermal-decomposition of magnetite (Fe_3O_4) nanoparticles. *Mater. Sci. Pol.*, 31(2), 264–268. https://doi.org/10.2478/s13536-012-0100-6
25. Patra, J. K. & Baek, K. (2017). Green biosynthesis of magnetic iron oxide (Fe_3O_4) nanoparticles using the aqueous extracts of food processing wastes under photo-catalyzed condition and investigation of their antimicrobial and antioxidant activity. *J. Photochem. Photobiol. B Biol.*, 173, 291–300. https://doi.org/10.1016/j.jphotobiol.2017.05.045
26. Janot, R. & Guérard, D. (2002). One-step synthesis of maghemite nanometric powers by ball milling. *J. Alloys. Compd.*, 333, 302–307.
27. Karimi, Z. et al. (2013). Nano-magnetic particles used in biomedicine: Core and coating materials. *Mater. Sci. Eng. C Mater. Biol. Appl.*, 33(5), 2465–2475. https://doi.org/10.1016/j.msec.2013.01.045
28. Bashir, M. et al. (2015). *Effect of PH on ferromagnetic iron oxide nanoparticles*. UK: Elsevier Ltd., 2(10), 5664–5668. https://doi.org/10.1016/j.matpr.2015.11.106
29. Ewijk, G. A. et al. (1999). Convenient preparation methods for magnetic colloids. *J. Magn. Magn. Mater.*, 201(1–3), 31–33. https://doi.org/10.1016/S0304-8853(99)00080-3
30. Daou, T. J. et al. (2006). Hydrothermal synthesis of monodisperse magnetite nanoparticles. *Chem. Mater.*, 18(18), 4399–4404. https://doi.org/10.1021/cm060805r
31. Kang, Y. S. et al. (1996). Synthesis and characterization of nanometer-size Fe_3O_4 and γ-Fe_2O_3 particles. *Chem. Mater.*, 8(9), 2209–2211. https://doi.org/10.1021/cm960157j
32. Saxena, N. & Singh, M. (2017). Efficient synthesis of superparamagnetic magnetite nanoparticles under air for biomedical applications. *J. Magn. Magn. Mater.*, 429, 166–176. https://doi.org/10.1016/j.jmmm.2017.01.031
33. Bepari, R. A. et al. (2017). Controlled synthesis of α- and γ-Fe_2O_3 nanoparticles via thermolysis of PVA gels and studies on α-Fe_2O_3 catalyzed styrene epoxidation. *J. Saudi. Chem. Soc.*, 21(1), S170–S178. https://doi.org/10.1016/j.jscs.2013.12.010
34. Layek, S. et al. (2011). Synthesis of γ–Fe_2O_3 nanoparticles with crystallographic and magnetic texture. *Int. J. Eng. Sci. Technol.*, 2(8), 33–39. https://doi.org/10.4314/ijest.v2i8.63778